Int. J. Solids Structures Vol. 30, No. 15, pp. 2071–2095, 1993
Printed in Great Britain

0020–7683/93 $6.00+ .00

SOLIDS WITH PERIODICALLY DISTRIBUTED CRACKS

S. NEMAT-NASSER and N. YU†
Center of Excellence for Advanced Materials, Department of Applied Mechanics and Engineering Sciences, 0411, 9500 Gilman Drive, University of California, San Diego, La Jolla, CA 92093, U.S.A.

and

M. HORI
Department of Civil Engineering, University of Tokyo, Bunkyo-ku, Tokyo 113, Japan

(*Received* 29 *April* 1992; *in revised form* 19 *December* 1992)

Abstract—A systematic method is presented for estimating the overall properties of solids with periodically distributed cracks. In view of the periodicity, the displacement, strain and stress fields of the cracked solid can be expressed in Fourier series. Elastic solids with periodically distributed flat voids are considered first. The results for cracks are then obtained by letting the thickness aspect ratio of the void approach zero. This limiting process is performed with care. The only approximation involved is the distribution of the homogenization eigenstrains, which is assumed to be piecewise constant. The estimate of overall elastic moduli, crack opening displacements and stress intensity factors eventually reduces to the calculation of several infinite series. The formulation is valid for elliptic as well as two-dimensional line (slit-like) cracks, and cracks with arbitrary shapes. It fully includes the interaction effects.

1. INTRODUCTION

The estimate of the overall properties of cracked solids has been considered by a number of authors. Bristow (1960) theoretically and experimentally studied solids with randomly distributed long rectangular (ribbon-like) and penny-shaped cracks. Fluid-filled penny-shaped cracks were later considered by Walsh (1969). In these early studies, the crack distribution was assumed to be dilute so that the interactions among cracks were ignored. For high crack densities, O'Connell and Budiansky (1974) and Budiansky and O'Connell (1976) have used the self-consistent method (SCM) to account for the interaction effects to a certain extent. Horii and Nemat-Nasser (1983) further included the effects of frictional sliding, crack closure, and load-induced anisotropy. Hoenig (1979) applied the SCM to nonrandom crack distributions. He presented the results when elliptic cracks are randomly distributed in planes parallel to a given plane (i.e. aligned cracks), and when the crack normals are parallel to a plane, but have otherwise randomly distributed orientations. Laws and Brockenbrough (1987) have summarized the self-consistent solutions for both random and nonrandom crack distributions.

The validity of SCM at high crack densities was questioned by Bruner (1976), Henyey and Pomphrey (1982), and Hashin (1988). Instead, they employed the differential scheme (DS) to take account of the crack interactions. This application of DS to cracked solids originated with Salganik (1973). The results obtained by DS usually indicate smaller stiffness degradation than that predicted by SCM. Nemat-Nasser and Hori (1988, 1990, 1993) have systematically presented and compared the results of randomly distributed and aligned penny-shaped as well as two-dimensional line (slit-like) cracks using dilute distribution, SCM, and DS.

Since the static elastic moduli of solids are related to the speeds of waves of low frequency (long wavelength), Hudson (1980, 1990; see also the references cited there) and Hudson and Knopoff (1989) have used the method of smoothing to formulate the problem of cracked solids for both randomly oriented and aligned dry and fluid-filled penny-shaped

† Present address: Department of Engineering Science and Mechanics, University of Tennessee, Knoxville, TN 37996, U.S.A.

cracks. The formulation is accurate to second order in the crack density parameter, though the number of cracks per unit volume must be small. The bounding of overall elasticity and compliance tensors is also derived from dynamic problems by Willis (1980a, b).

Benveniste (1986) has applied the Mori–Tanaka method (Mori and Tanaka, 1973) to calculate the overall elastic moduli of solids containing randomly distributed 2-D line cracks, under the plane stress condition. Aboudi and Benveniste (1987) studied the isotropic cracked solids under plane deformations by using the generalized self-consistent method, which accounted for the interaction effects by considering a single crack surrounded by the matrix material and then both embedded in the effective medium. This method has been proposed by Fröhlich and Sack (1946), and has been employed by Mackenzie (1950), Kerner (1956), Hermans (1967), van der Poel (1958), Smith (1974, 1975), Christensen and Lo (1979, 1986), and Christensen (1990) to study various void and inhomogeneity problems.

For 2-D line cracks, Delameter *et al.* (1975, 1977) have considered a doubly periodic rectangular array of cracks and have represented cracks as suitable distributions of dislocations. Horii and Sahasakmontri (1990) have applied the superposition technique to study the effect of crack interactions. Recently, Deng and Nemat-Nasser (1992) have obtained the exact solutions for an infinite row of collinear cracks, and using three different averaging techniques (dilute distribution, SCM, and DS) have estimated the overall moduli of elastic solids containing parallel and random distributions of crack arrays.

In this paper, the problem of the effect of a periodic distribution of cracks on the overall properties, is studied. An infinitely extended solid is considered which contains periodically distributed cracks in such a manner that the solid may be regarded as a collection of unit cells of identical dimensions, each including one or more cracks of possibly arbitrary shapes; see Fig. 1. The elastic fields in a unit cell then represent those of the infinite periodic structure. The solution strategy can be divided into three steps. An *inclusion* problem is solved first. The solution gives the perturbation elastic fields due to an *arbitrary* eigenstrain field prescribed within a *homogeneous* unit cell. Next, an *inhomogeneity* (here, a void) problem is considered, and the unit cell is replaced by an equivalent *homogeneous* unit cell with *suitable* homogenization eigenstrains introduced within the void region such that the resulting stress and strain fields are identical with those of the original cell which contains the voids. This inhomogeneity problem then reduces to an inclusion problem and

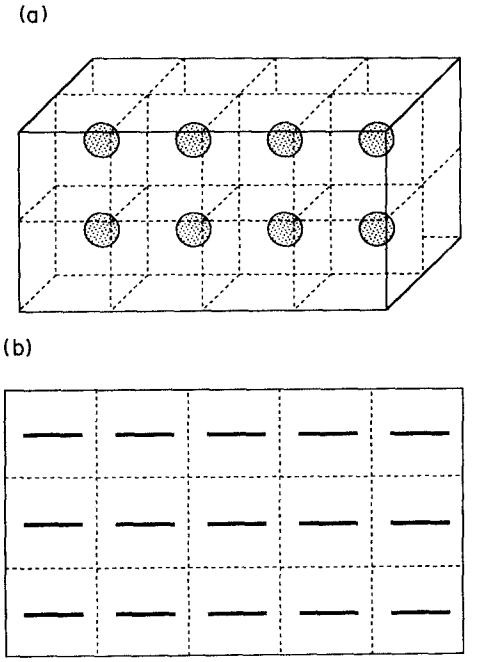

Fig. 1. (a) Periodically distributed penny-shaped cracks; (b) periodically distributed two-dimensional line cracks.

therefore can be solved; this is the counterpart of the Eshelby (1957) problem of an unbounded solid. Finally, a crack is treated as a void, one of whose dimensions becomes vanishingly small. Thus a limiting process is used to obtain the solution for the corresponding crack problem.

2. OVERALL MODULI

2.1. *General formulation*

Consider a unit cell, U, in the shape of a parallelepiped with dimensions $2a_i$, measured along the coordinate axes, x_i, $i = 1, 2, 3$. Denote by Ω the region occupied by a flat void within the cell. The void may be a flat ellipsoid or a flat elliptic cylinder with dimensions $2c_i$ (or, indeed, any arbitrary shape); see Fig. 2(a, b). The estimate of the overall elastic moduli of solids with such periodic microstructure can be obtained from the analysis presented by Nemat-Nasser and Taya (1981, 1985), Nemat-Nasser *et al.* (1982), and Iwakuma and Nemat-Nasser (1983) which is briefly reviewed below.

Let the material of the cell be linearly elastic with elasticity tensor $\mathbf{C}$. First, an *inclusion* problem is considered, where within a homogeneous unit cell (without a void), arbitrary eigenstrains, $\boldsymbol{\varepsilon}^*(\mathbf{x})$, are prescribed, resulting in the perturbation strains $\boldsymbol{\varepsilon}^p(\mathbf{x})$ and associated displacements $\mathbf{u}^p(\mathbf{x})$ and stresses $\boldsymbol{\sigma}^p(x)$. The geometric periodicity implies the periodicity of

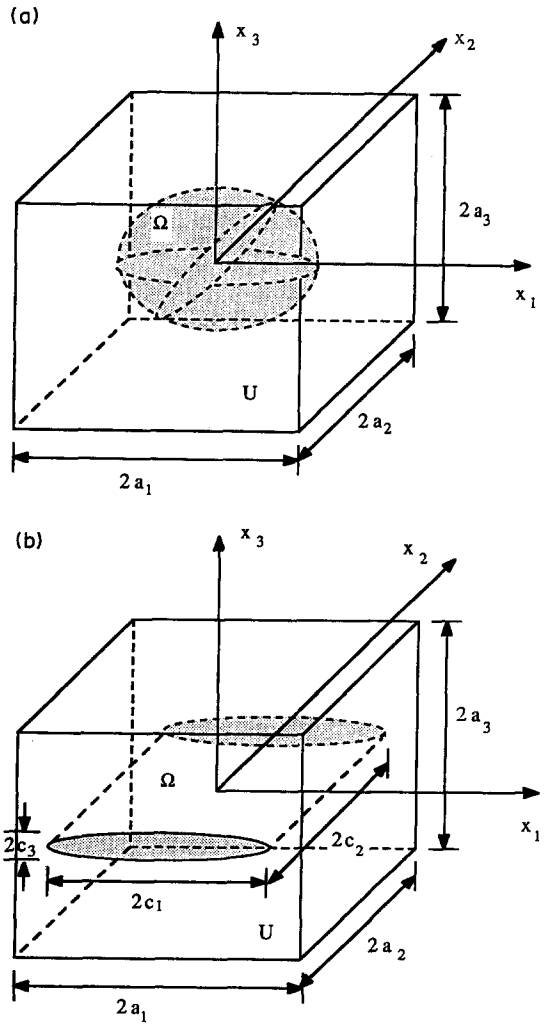

Fig. 2. Unit cell containing (a) a flat ellipsoidal void, and (b) a flat elliptic-cylindrical void.

perturbation fields $\mathbf{u}^{\mathrm{p}}(\mathbf{x})$, $\boldsymbol{\varepsilon}^{\mathrm{p}}(\mathbf{x})$, and $\boldsymbol{\sigma}^{\mathrm{p}}(\mathbf{x})$, as well as that of the eigenstrain, $\boldsymbol{\varepsilon}^*(\mathbf{x})$. It follows that $\mathbf{u}^{\mathrm{p}}(\mathbf{x})$ and $\boldsymbol{\varepsilon}^*(\mathbf{x})$ can be expressed in the Fourier series:

$$\mathbf{u}^{\mathrm{p}}(\mathbf{x}) = \sum_{\xi}^{\pm\infty\prime} \hat{\mathbf{u}}^{\mathrm{p}}(\boldsymbol{\xi}) \exp(i\boldsymbol{\xi}\cdot\mathbf{x}), \tag{1}$$

$$\begin{aligned}\boldsymbol{\varepsilon}^*(\mathbf{x}) &= \sum_{\xi}^{\pm\infty} \hat{\boldsymbol{\varepsilon}}^*(\boldsymbol{\xi}) \exp(i\boldsymbol{\xi}\cdot\mathbf{x}) \\ &= \langle\boldsymbol{\varepsilon}^*(\mathbf{x})\rangle_U + \sum_{\xi}^{\pm\infty\prime} \hat{\boldsymbol{\varepsilon}}^*(\boldsymbol{\xi}) \exp(i\boldsymbol{\xi}\cdot\mathbf{x}),\end{aligned} \tag{2}$$

where the angled brackets with the subscript U represent the volume average over U:

$$\xi_i = \frac{\pi n_i}{a_i}, \quad n_i = 0, \pm 1, \pm 2, \ldots \ (i \text{ not summed}), \tag{3}$$

and the prime on the summation sign means that the term associated with $\boldsymbol{\xi} = \mathbf{0}$ is excluded, since $\hat{\mathbf{u}}^{\mathrm{p}}(\mathbf{0})$ represents a rigid body translation, and the homogeneous part of eigenstrains, $\hat{\boldsymbol{\varepsilon}}^*(\mathbf{0})$, yields a linear displacement field which is not periodic and is dealt with separately (see below). The Fourier coefficients $\hat{\mathbf{u}}^{\mathrm{p}}(\boldsymbol{\xi})$ and $\hat{\boldsymbol{\varepsilon}}^*(\boldsymbol{\xi})$ are

$$\hat{\mathbf{u}}^{\mathrm{p}}(\boldsymbol{\xi}) = \frac{1}{V_U}\int_U \mathbf{u}^{\mathrm{p}}(\mathbf{x}) \exp(-i\boldsymbol{\xi}\cdot\mathbf{x})\, \mathrm{d}V_x, \tag{4}$$

$$\hat{\boldsymbol{\varepsilon}}^*(\boldsymbol{\xi}) = \frac{1}{V_U}\int_U \boldsymbol{\varepsilon}^*(\mathbf{x}) \exp(-i\boldsymbol{\xi}\cdot\mathbf{x})\, \mathrm{d}V_x, \tag{5}$$

with V_U being the volume of the unit cell.

The equilibrium requires

$$\nabla\cdot\{\mathbf{C}:[\boldsymbol{\varepsilon}^{\mathrm{p}}(\mathbf{x}) - \boldsymbol{\varepsilon}^*(\mathbf{x})]\} = \mathbf{0} \quad \text{in } U. \tag{6}$$

Substitution of (1) and (2) into (6) gives (Nemat-Nasser and Taya, 1981)

$$\boldsymbol{\varepsilon}^{\mathrm{p}}(\mathbf{x}) \equiv \mathbf{S}^{\mathrm{p}}(\mathbf{x};\boldsymbol{\varepsilon}^*) = \sum_{\xi}^{\pm\infty\prime} \hat{\mathbf{S}}(\boldsymbol{\xi}) : \left[\frac{1}{V_U}\int_U \boldsymbol{\varepsilon}^*(\mathbf{y}) \exp(i\boldsymbol{\xi}\cdot(\mathbf{x}-\mathbf{y}))\, \mathrm{d}V_y\right], \tag{7}$$

where

$$\hat{\mathbf{S}}(\boldsymbol{\xi}) = sym\,[\boldsymbol{\xi}\otimes(\boldsymbol{\xi}\cdot\mathbf{C}\cdot\boldsymbol{\xi})^{-1}\otimes\boldsymbol{\xi}] : \mathbf{C}, \tag{8}$$

and *sym* stands for the symmetric part of the corresponding fourth-order tensor; i.e. $sym\ \hat{S}_{ijkl} = (\hat{S}_{ijkl} + \hat{S}_{ijlk} + \hat{S}_{jikl} + \hat{S}_{jilk})/4$. Note that (8) necessarily requires $\boldsymbol{\xi} \neq \mathbf{0}$. Thus the homogeneous part of eigenstrains, $\langle\boldsymbol{\varepsilon}^*(\mathbf{x})\rangle_U$ $(= \hat{\boldsymbol{\varepsilon}}^*(\mathbf{0}))$, has no contributions to the periodic perturbation strain, $\boldsymbol{\varepsilon}^{\mathrm{p}}(\mathbf{x})$. For the case of an isotropic matrix, tensor $\hat{\mathbf{S}}(\boldsymbol{\xi})$ reduces to

$$\hat{\mathbf{S}}(\boldsymbol{\xi}) = 2\,sym\,(\bar{\boldsymbol{\xi}}\otimes\mathbf{1}^{(2)}\otimes\bar{\boldsymbol{\xi}}) - \frac{1}{1-\nu}\bar{\boldsymbol{\xi}}\otimes\bar{\boldsymbol{\xi}}\otimes\bar{\boldsymbol{\xi}}\otimes\bar{\boldsymbol{\xi}} + \frac{\nu}{1-\nu}\bar{\boldsymbol{\xi}}\otimes\bar{\boldsymbol{\xi}}\otimes\mathbf{1}^{(2)}, \tag{9}$$

where $\mathbf{1}^{(2)}$ is the second-order unit tensor, ν is the Poisson ratio, and

$$\bar{\xi} = \frac{\xi}{|\xi|} = \frac{\xi}{\sqrt{\xi \cdot \xi}}. \tag{10}$$

The *integral* operator $\mathbf{S}^{\mathrm{p}}(\mathbf{x}; \boldsymbol{\varepsilon}^*)$ defined in (7) relates an arbitrary eigenstrain field $\boldsymbol{\varepsilon}^*(\mathbf{x})$ to the corresponding peturbation strain $\boldsymbol{\varepsilon}^{\mathrm{p}}(\mathbf{x})$ and therefore functions as the Eshelby's tensor (Eshelby, 1957). The differences are that the Eshelby's results are applied to a single inclusion embedded in an infinitely extended body resulting in an algebraic relation between the eigenstrain and the perturbation strain, while $\mathbf{S}^{\mathrm{p}}(\mathbf{x}; \boldsymbol{\varepsilon}^*)$ is an integral operator associated with a periodic structure. When the inclusion is ellipsoidal and the material is isotropic, the constant Eshelby's tensor depends on only the Poisson ratio of the material and the aspect ratios of the inclusion whereas $\mathbf{S}^{\mathrm{p}}(\mathbf{x}; \boldsymbol{\varepsilon}^*)$ in the case of an isotropic matrix reduces to three integral operators which are dependent on the shape of the inclusion [see eqns (7) and (9)].

The *periodic* perturbation stress is obtained by generalized Hooke's law:

$$\boldsymbol{\sigma}^{\mathrm{p}}(\mathbf{x}) = \mathbf{C} : [\boldsymbol{\varepsilon}^{\mathrm{p}}(\mathbf{x}) - (\boldsymbol{\varepsilon}^*(\mathbf{x}) - \langle \boldsymbol{\varepsilon}^*(\mathbf{x}) \rangle_U)] \quad \text{in } U, \tag{11}$$

where $\boldsymbol{\varepsilon}^*(\mathbf{x}) - \langle \boldsymbol{\varepsilon}^*(\mathbf{x}) \rangle_U$ is the periodic part of the eigenstrain field. The completeness and uniqueness of the solution of the equations of equilibrium, (7), are ensured by the boundary conditions of the unit cell (see Appendix).

Next, the *inhomogeneity* (void) problem is considered. In the absence of any voids, the stress field would be uniform, $\boldsymbol{\sigma}(\mathbf{x}) = \boldsymbol{\sigma}^\circ$, when the overall homogeneous stress $\boldsymbol{\sigma}^\circ$ is prescribed. The presence of voids, however, disturbs the uniformity of the stress field and results in perturbation stress field, $\boldsymbol{\sigma}^{\mathrm{p}}(\mathbf{x})$. The total stress and strain fields are

$$\boldsymbol{\sigma}(\mathbf{x}) = \boldsymbol{\sigma}^\circ + \boldsymbol{\sigma}^{\mathrm{p}}(\mathbf{x}), \tag{12}$$

$$\boldsymbol{\varepsilon}(\mathbf{x}) = \boldsymbol{\varepsilon}^\circ + \boldsymbol{\varepsilon}^{\mathrm{p}}(\mathbf{x}), \tag{13}$$

where $\boldsymbol{\varepsilon}^\circ$ and $\boldsymbol{\varepsilon}^{\mathrm{p}}(\mathbf{x})$ are the corresponding homogeneous and periodic parts of the total strain field, respectively. One can replace this heterogeneous unit cell by an equivalent *homogeneous* unit cell of constant elasticity tensor $\mathbf{C}$ and introduce a *suitable* eigenstrain field, $\boldsymbol{\varepsilon}^*(\mathbf{x})$, within Ω such that the following *consistency condition* is satisfied:

$$\begin{aligned} \boldsymbol{\sigma}(\mathbf{x}) &= \boldsymbol{\sigma}^\circ + \boldsymbol{\sigma}^{\mathrm{p}}(\mathbf{x}) \\ &= \boldsymbol{\sigma}^\circ + \mathbf{C} : [\boldsymbol{\varepsilon}^{\mathrm{p}}(\mathbf{x}) - (\boldsymbol{\varepsilon}^*(\mathbf{x}) - \langle \boldsymbol{\varepsilon}^*(\mathbf{x}) \rangle_U] = \mathbf{0} \quad \text{in } \Omega, \end{aligned} \tag{14}$$

where (11) is used. In this manner $\boldsymbol{\varepsilon}^*(\mathbf{x})$ is calculated so that the stress-free condition within Ω is maintained by homogenization. Thus the inhomogeneity problem reduces to an inclusion problem.

The overall compliance tensor, $\bar{\mathbf{D}}$, is defined by

$$\langle \boldsymbol{\varepsilon}(\mathbf{x}) \rangle_U = \boldsymbol{\varepsilon}^\circ \equiv \bar{\mathbf{D}} : \boldsymbol{\sigma}^\circ = \mathbf{D} : \boldsymbol{\sigma}^\circ + \langle \boldsymbol{\varepsilon}^*(\mathbf{x}) \rangle_U. \tag{15}$$

One concludes that though the homogeneous part of the eigenstrain, $\langle \boldsymbol{\varepsilon}^*(\mathbf{x}) \rangle_U$, does not contribute to the periodic perturbation strains or stresses, it does affect the homogeneous stress and strain fields through (15). Also note that the volume average of $\boldsymbol{\varepsilon}^*(\mathbf{x})$, rather than its exact distribution, is needed in calculating $\bar{\mathbf{D}}$. As will be shown, one may therefore use crude approximations for $\boldsymbol{\varepsilon}^*(\mathbf{x})$ and yet obtain accurate estimates of $\bar{\mathbf{D}}$. Thus, substituting (7) into (14) and taking the volume average over Ω, we obtain

$$\boldsymbol{\sigma}^\circ + \sum_{\xi}^{\pm\infty\prime} \mathbf{C} : \hat{\mathbf{S}}(\xi) : [\langle \boldsymbol{\varepsilon}^*(\mathbf{y}) \exp(-i\xi \cdot \mathbf{y}) \rangle_U g(\xi)] - \mathbf{C} : (\langle \boldsymbol{\varepsilon}^*(\mathbf{x}) \rangle_\Omega - \langle \boldsymbol{\varepsilon}^*(\mathbf{x}) \rangle_U) = \mathbf{0}, \tag{16}$$

where

$$g(\xi) = \frac{1}{V_\Omega}\int_\Omega \exp(i\xi\cdot\mathbf{x})\,dV_x. \tag{17}$$

In order to solve the integral equation (16) in the simplest possible manner, an approximation is made by assuming the distribution of eigenstrains to be uniform within Ω:

$$\boldsymbol{\varepsilon}^*(\mathbf{x}) = H(\Omega)\boldsymbol{\varepsilon}^{*\circ}, \tag{18}$$

where $\boldsymbol{\varepsilon}^{*\circ}$ is constant and $H(\Omega)$ is the Heaviside step function. That is, we replace $\boldsymbol{\varepsilon}^*(\mathbf{y})$ by its average value, $\langle\boldsymbol{\varepsilon}^*(\mathbf{y})\rangle_\Omega$, in (16). Combination of (16) and (18) now gives

$$\boldsymbol{\varepsilon}^{*\circ} = \left[(1-f)\mathbf{C} - \sum_{\xi}^{\pm\infty\prime} fg(-\xi)g(\xi)\mathbf{C}:\hat{\mathbf{S}}(\xi)\right]^{-1}:\boldsymbol{\sigma}^\circ, \tag{19}$$

where $f = V_\Omega/V_U$ is the void volume fraction. It follows from (15) and (19) that

$$\bar{\mathbf{D}} = \mathbf{D}+\mathbf{H}, \tag{20}$$

where

$$\mathbf{H} = f\left[(1-f)\mathbf{C} - \sum_{\xi}^{\pm\infty\prime} fg(-\xi)g(\xi)\mathbf{C}:\hat{\mathbf{S}}(\xi)\right]^{-1}. \tag{21}$$

Note that the effect of void geometry is embedded in the geometrical parameter $g(\xi)$, and is separated from the elastic properties of the material which are included in the $\hat{\mathbf{S}}$-tensor.

Now, a crack can be viewed as a limiting case of a void, one of whose dimensions, say, c_3, is vanishingly small, compared with the other two dimensions. Then the overall compliance tensor becomes

$$\bar{\mathbf{D}} = \mathbf{D}+\lim_{\beta\to 0}\mathbf{H}, \tag{22}$$

where $\beta = c_3/c_1$ is the thickness aspect ratio of the void. It will be shown below that the right-hand side of (19) is of the order of $1/\beta$ and can be rewritten as

$$\boldsymbol{\varepsilon}^{*\circ} = \frac{1}{\beta}(\mathbf{U}^{\mathrm{p}})^{-1}:\boldsymbol{\sigma}^\circ, \tag{23}$$

where

$$(\mathbf{U}^{\mathrm{p}})^{-1} = \beta\left[(1-f)\mathbf{C} - \sum_{\xi}^{\pm\infty\prime} fg(-\xi)g(\xi)\mathbf{C}:\hat{\mathbf{S}}(\xi)\right]^{-1} \tag{24}$$

is a fourth-order tensor of $O(1)$. This tensor will be used in calculating the crack opening displacement (COD) and stress intensity factor (SIF) of solids containing periodically distributed cracks (Section 3). As is seen from (23), as $\beta\to 0$, $\boldsymbol{\varepsilon}^{*\circ}$ becomes unbounded. However, $\lim_{\beta\to 0}\mathbf{H}$ still exists and is bounded, or equivalently, the average $\langle\boldsymbol{\varepsilon}^*(\mathbf{x})\rangle_U$ remains finite. This limiting process is discussed in detail in the next subsection. One also notes that, at this stage, the shape of the crack need not be specified. Thus the formulation is valid for cracks with arbitrary shapes.

2.2. *Elliptic cracks*

As an illustration, consider a flat ellipsoidal void with semi-axes $c_1 \geqslant c_2 > c_3$ [see Fig. 2(a)]. For an isotropic matrix,

$$\mathbf{C} = \mu\left[\frac{2\nu}{1-2\nu}\mathbf{1}^{(2)} \otimes \mathbf{1}^{(2)} + 2\mathbf{1}^{(4s)}\right], \tag{25}$$

where μ is the shear modulus and $\mathbf{1}^{(4s)}$ is the fourth-order symmetric unit tensor with components

$$1^{(4s)}_{ijkl} = \tfrac{1}{2}(\delta_{ik}\delta_{jl} + \delta_{il}\delta_{jk}). \tag{26}$$

Combination of (9) and (25) gives

$$\mathbf{C}:\hat{\mathbf{S}}(\xi) = \frac{2\mu}{1-\nu}\left[\frac{\nu^2}{1-2\nu}\mathbf{1}^{(2)} \otimes \mathbf{1}^{(2)} + \nu(\mathbf{1}^{(2)} \otimes \bar{\xi} \otimes \bar{\xi} + \bar{\xi} \otimes \bar{\xi} \otimes \mathbf{1}^{(2)}) - \bar{\xi} \otimes \bar{\xi} \otimes \bar{\xi} \otimes \bar{\xi} + 2(1-\nu)\, sym\,(\bar{\xi} \otimes \mathbf{1}^{(2)} \otimes \bar{\xi})\right]. \tag{27}$$

Now, define

$$s^{pq} \equiv \sum_{\xi}^{\pm\infty\prime} g(-\xi)g(\xi)(\bar{\xi}_1^2)^p(\bar{\xi}_2^2)^q \quad \text{for } p, q = 0, 1, 2. \tag{28}$$

From (25) and (27), one readily obtains

$$\left[(1-f)\mathbf{C} - \sum_{\xi}^{\pm\infty\prime} fg(-\xi)g(\xi)\mathbf{C}:\hat{\mathbf{S}}(\xi)\right] = \beta[\mathbf{U}^p] = \begin{bmatrix}[\mathbf{K}^1] & [\mathbf{0}] \\ [\mathbf{0}] & [\mathbf{K}^2]\end{bmatrix}, \tag{29}$$

where $[\mathbf{0}]$ is the null matrix, $[\mathbf{K}^1]$ has the form

$$[\mathbf{K}^1] = \frac{2\mu}{1-\nu}\begin{bmatrix} 1 & \nu & O(\beta) \\ & 1 & O(\beta) \\ sym & & (\beta d)(2s^{11} + s^{20} + s^{02}) \end{bmatrix}, \tag{30}$$

$[\mathbf{K}^2]$ is a diagonal matrix with the following *tensorial* components:

$$K^2_{2323} = (\beta d)\left(\frac{2\mu}{1-\nu}\right)\left[\left(\frac{1-\nu}{2}\right)s^{10} + s^{01} - s^{11} - s^{02}\right], \tag{31}$$

$$K^2_{3131} = (\beta d)\left(\frac{2\mu}{1-\nu}\right)\left[\left(\frac{1-\nu}{2}\right)s^{01} + s^{10} - s^{11} - s^{20}\right], \tag{32}$$

$$K^2_{1212} = O(1), \tag{33}$$

and $d = f/\beta$. In the derivation of (29)–(33), identities

$$\bar{\xi}_1^2 + \bar{\xi}_2^2 + \bar{\xi}_3^2 = 1, \tag{34}$$

$$\sum_{\xi}^{\pm\infty\prime} fg(-\xi)g(\xi) = 1 - f \tag{35}$$

are used. The latter follows from the fact that $fg(-\xi)$ is the Fourier coefficient of the Heaviside step function $H(\Omega)$,

$$\frac{1}{V_U}\int_U H(\Omega)\exp(-i\xi\cdot\mathbf{x})\,dV_x = fg(-\xi). \tag{36}$$

Calculating the average of $H(\Omega)$ over Ω, we obtain

$$\langle H(\Omega)\rangle_\Omega = \sum_{\xi}^{\pm\infty} fg(-\xi)g(\xi) = 1, \tag{37}$$

which leads to (35).

By inverting matrices $[\mathbf{K}^1]$ and $[\mathbf{K}^2]$ note that, as β approaches 0, the components of the **H**-tensor in (21) all vanish, except for

$$H_{3333} = \left(\frac{1-\nu^2}{E}\right)(2s^{11}+s^{20}+s^{02})^{-1}, \tag{38}$$

$$H_{2323} = \frac{1}{4\mu}\left[s^{10}+\left(\frac{2}{1-\nu}\right)(s^{01}-s^{11}-s^{02})\right]^{-1}, \tag{39}$$

$$H_{3131} = \frac{1}{4\mu}\left[s^{01}+\left(\frac{2}{1-\nu}\right)(s^{10}-s^{11}-s^{20})\right]^{-1}. \tag{40}$$

It follows that the overall Young's modulus $\bar{E}_3$ and shear moduli $\bar{\mu}_{23}$ and $\bar{\mu}_{31}$, are given by

$$\bar{E}_3/E = [1+(1-\nu^2)(2s^{11}+s^{20}+s^{02})^{-1}]^{-1}, \tag{41}$$

$$\bar{\mu}_{23}/\mu = \left\{1+\left(\frac{1-\nu}{2}\right)\left[\left(\frac{1-\nu}{2}\right)s^{10}+s^{01}-s^{11}-s^{02}\right]^{-1}\right\}^{-1}, \tag{42}$$

$$\bar{\mu}_{31}/\mu = \left\{1+\left(\frac{1-\nu}{2}\right)\left[s^{10}+\left(\frac{1-\nu}{2}\right)s^{01}-s^{11}-s^{20}\right]^{-1}\right\}^{-1}. \tag{43}$$

Furthermore, as $\beta\to 0$, the void volume fraction f also tends to zero. A suitable parameter which measures the crack density is then defined by

$$f^* \equiv \lim_{\substack{\beta\to 0\\ f\to 0}} \frac{f}{(\frac{4}{3}\pi)\beta} = \frac{1}{8}\left(\frac{c_1}{a_1}\right)^3 \frac{\alpha}{\gamma_2\gamma_3}, \tag{44}$$

where $\alpha = c_2/c_1$ and $\gamma_i = a_i/a_1$, $i = 2, 3$. This parameter explicitly includes the factors of the crack shape (α), normalized crack size (c_1/a_1), and crack spacing (γ_i). It is the equivalent of the crack density parameter introduced by Budiansky and O'Connell (1976).

The estimate of the overall moduli, (41)–(43), now reduces to the calculation of infinite series s^{pq} for $\beta\to 0$. For an ellipsoidal void, the geometrical parameter $g(\xi)$ is given by

$$g(\xi) = \frac{1}{V_\Omega}\int_\Omega \exp(i\xi\cdot\mathbf{x})\,dV_x = \frac{3(\sin\eta-\eta\cos\eta)}{\eta^3}, \tag{45}$$

where

$$\eta = \sqrt{(\xi_1 c_1)^2+(\xi_2 c_2)^2+(\xi_3 c_3)^2}. \tag{46}$$

Thus, one finds as $\beta\to 0$, that $g(\xi)$ reduces to

$$g^*(\zeta) \equiv \lim_{\beta \to 0} g(\xi) = \frac{3(\sin \zeta - \zeta \cos \zeta)}{\zeta^3}, \tag{47}$$

where instead of the three-dimensional vector ξ, the two-dimensional vector ζ with components

$$\zeta_i = \frac{\pi n_i}{a_i} \quad \text{for } i = 1,2 \ (i \text{ not summed}) \tag{48}$$

is used, and

$$\zeta = |\zeta| = \pi \left(\frac{c_1}{a_1}\right) \sqrt{n_1^2 + (\alpha n_2/\gamma_2)^2}. \tag{49}$$

With the help of the following identities:

$$\sum_n^{\pm\infty} \frac{M^2}{M^2+n^2} = (\pi M) \coth (\pi M), \tag{50}$$

$$\sum_n^{\pm\infty} \left(\frac{M^2}{M^2+n^2}\right)^2 = \tfrac{1}{2}[(\pi M) \coth (\pi M) + (\pi M)^2 \operatorname{csch}^2 (\pi M)], \tag{51}$$

with M being a constant, one obtains

$$\begin{aligned} s^{10} &= \sum_{\zeta}^{\pm\infty}{}' g^*(\zeta) g^*(-\zeta) \frac{\zeta_1^2}{\zeta_1^2+\zeta_2^2} \sum_{\zeta_3}^{\pm\infty} \frac{\zeta_1^2+\zeta_2^2}{\zeta_1^2+\zeta_2^2+\zeta_3^2} \\ &= \sum_{\zeta}^{\pm\infty}{}' g^*(\zeta) g^*(-\zeta) \bar{\zeta}_1^2 (\zeta^* \coth \zeta^*), \end{aligned} \tag{52}$$

where

$$\bar{\zeta}_i = \frac{\zeta_i}{|\zeta|} = \frac{n_i}{\gamma_i \sqrt{n_1^2 + (n_2/\gamma_2)^2}}, \tag{53}$$

$$\zeta^* = a_3 |\zeta| = \pi \gamma_3 \sqrt{n_1^2 + \left(\frac{n_2}{\gamma_2}\right)^2}. \tag{54}$$

Similarly,

$$s^{01} = \sum_{\zeta}^{\pm\infty}{}' g^*(\zeta) g^*(-\zeta) \bar{\zeta}_2^2 (\zeta^* \coth \zeta^*), \tag{55}$$

$$s^{11} = \frac{1}{2} \sum_{\zeta}^{\pm\infty}{}' g^*(\zeta) g^*(-\zeta) (\bar{\zeta}_1 \bar{\zeta}_2)^2 (\zeta^* \coth \zeta^* + \zeta^{*2} \operatorname{csch}^2 \zeta^*), \tag{56}$$

$$s^{20} = \frac{1}{2} \sum_{\zeta}^{\pm\infty}{}' g^*(\zeta) g^*(-\zeta) \bar{\zeta}_1^4 (\zeta^* \coth \zeta^* + \zeta^{*2} \operatorname{csch}^2 \zeta^*), \tag{57}$$

$$s^{02} = \frac{1}{2} \sum_{\zeta}^{\pm\infty\prime} g^*(\zeta) g^*(-\zeta) \bar{\zeta}_2^4 (\zeta^* \coth \zeta^* + \zeta^{*2} \operatorname{csch}^2 \zeta^*). \tag{58}$$

2.3. *Two-dimensional line cracks*

For the unit cell containing an elliptic-cylindrical void as shown in Fig. 2(b), the geometrical parameter $g(\xi)$ is given by

$$g(\xi) = \frac{2J_1(c_1\sqrt{\xi_1^2 + (\beta\xi_3)^2})}{c_1\sqrt{\xi_1^2 + (\beta\xi_3)^2}} \left[\frac{\sin(c_2\xi_2)}{(c_2\xi_2)}\right]. \tag{59}$$

As the thickness aspect ratio β $(= c_3/c_1)$ goes to zero, the flat void collapses into a 2-D line crack. Further, if one assumes that the cracks extend indefinitely along the x_2-direction with $c_2 = a_2$, a plane strain condition is then obtained. The corresponding $g(\xi)$ becomes

$$g^*(\zeta) \equiv \lim_{\beta \to 0} g(\xi) = \frac{2J_1(\pi n_1 c_1/a_1)}{(\pi n_1 c_1/a_1)} \frac{\sin(\pi n_2)}{(\pi n_2)}. \tag{60}$$

Accordingly, the infinite series s^{pq} become

$$s^{10} = \sum_{n_1 = \pm 1}^{\pm\infty} \frac{4J_1^2(\pi n_1 c_1/a_1)}{(\pi n_1 c_1/a_1)^2} (\pi n_1 \gamma_3) \coth(\pi n_1 \gamma_3), \tag{61}$$

$$s^{20} = \sum_{n_1 = \pm 1}^{\pm\infty} \frac{2J_1^2(\pi n_1 c_1/a_1)}{(\pi n_1 c_1/a_1)^2} [(\pi n_1 \gamma_3) \coth(\pi n_1 \gamma_3) + (\pi n_1 \gamma_3)^2 \operatorname{csch}^2(\pi n_1 \gamma_3)], \tag{62}$$

with all other elements being zero. Thus from (41)—(43), the overall moduli for a solid with periodically distributed 2-D line cracks are given by

$$\bar{E}_3/E = \left[1 + \left(\frac{1-\nu^2}{s^{20}}\right)\right]^{-1}, \tag{63}$$

$$\bar{\mu}_{23}/\mu = \left(1 + \frac{1}{s^{10}}\right)^{-1}, \tag{64}$$

$$\bar{\mu}_{31}/\mu = \left[1 + \left(\frac{1-\nu}{2}\right)(s^{10} - s^{20})^{-1}\right]^{-1}, \tag{65}$$

and the crack density parameter, f^*, is defined by

$$f^* \equiv \lim_{\substack{\beta \to 0 \\ f \to 0}} \frac{f}{\pi\beta} = \frac{1}{4\gamma_3} \left(\frac{c_1}{a_1}\right)^2. \tag{66}$$

It is noted that in this case the effect of normalized crack size (c_1/a_1) is separated from the effect of crack spacing (γ_3) in the calculation of infinite series s^{10} and s^{20}. We also emphasize that the results for 2-D line cracks can be readily obtained from that of the elliptic cracks provided that a suitable $g^*(\xi)$ is calculated.

2.4. *Piecewise constant eigenstrain distribution*

From (15), one observes that to estimate the overall elastic moduli of a solid with periodically distributed cracks, it is necessary to determine the volume average of eigenstrains, $\langle \boldsymbol{\varepsilon}^*(\mathbf{x}) \rangle_U$. However, one also learns from (16) that in order to calculate $\langle \boldsymbol{\varepsilon}^*(\mathbf{x}) \rangle_U$ exactly, one needs to know the exact distribution of $\boldsymbol{\varepsilon}^*(\mathbf{x})$. It turns out that the constant

eigenstrain approximation, (18), is extremely accurate. To check this, we consider a refinement by assuming a piecewise constant distribution of eigenstrains. That is, we set

$$\boldsymbol{\varepsilon}^*(\mathbf{x}) = \sum_{j=1}^{n} H(\Omega_j)\boldsymbol{\varepsilon}^{*j}, \tag{67}$$

where $\boldsymbol{\varepsilon}^{*j}$ ($j = 1, 2, \ldots, n$) are constant tensors; Ω_j are the subdivisions of Ω and

$$\Omega = \bigcup_{j=1}^{n} \Omega_j.$$

From (7), the average perturbation strain over Ω_i, $\langle \boldsymbol{\varepsilon}^p(\mathbf{x})\rangle_{\Omega_i}$, is given by

$$\langle \boldsymbol{\varepsilon}^p(\mathbf{x})\rangle_{\Omega_i} = \sum_{j=1}^{n} f_j \sum_{\boldsymbol{\xi}}^{\pm\infty\prime} g_j(-\boldsymbol{\xi}) g_i(\boldsymbol{\xi}) \hat{\mathbf{S}}(\boldsymbol{\xi}) : \boldsymbol{\varepsilon}^{*j} \quad \text{for } i = 1, 2, \ldots, n, \tag{68}$$

where

$$f_j = V_{\Omega_j}/V_U \quad \text{and } g_i(\boldsymbol{\xi}) = \frac{1}{V_{\Omega_i}} \int_{\Omega_i} \exp(i\boldsymbol{\xi}\cdot\mathbf{x})\, \mathrm{d}V_x. \tag{69}$$

The average consistency condition, (16), must now be satisfied in each Ω_i. This leads to a system of linear equations:

$$\sum_{j=1}^{n} \mathbf{K}^{ij} : \boldsymbol{\varepsilon}^{*j} = \boldsymbol{\sigma}^{\circ} \quad \text{in } \Omega_i \ (i = 1, 2, \ldots, n), \tag{70}$$

where

$$\mathbf{K}^{ii} = (1 - f_i)\mathbf{C} - f_i \sum_{\boldsymbol{\xi}}^{\pm\infty\prime} g_i(-\boldsymbol{\xi}) g_i(\boldsymbol{\xi}) \mathbf{C} : \hat{\mathbf{S}}(\boldsymbol{\xi}) \quad \text{for } i = j, \tag{71a}$$

$$\mathbf{K}^{ij} = -f_j\mathbf{C} - f_j \sum_{\boldsymbol{\xi}}^{\pm\infty\prime} g_j(-\boldsymbol{\xi}) g_i(\boldsymbol{\xi}) \mathbf{C} : \hat{\mathbf{S}}(\boldsymbol{\xi}) \quad \text{for } i \neq j. \tag{71b}$$

Following the procedures outlined in Subsection 2.2 and noting that

$$\sum_{\boldsymbol{\xi}}^{\pm\infty\prime} f_i g_i(-\boldsymbol{\xi}) g_i(\boldsymbol{\xi}) = 1 - f_i, \tag{72a}$$

$$\sum_{\boldsymbol{\xi}}^{\pm\infty\prime} f_j g_j(-\boldsymbol{\xi}) g_i(\boldsymbol{\xi}) = -f_j \quad \text{for } i \neq j, \tag{72b}$$

one finds that as $\beta \to 0$, for periodically distributed elliptic cracks (70) becomes

$$\sum_{j=1}^{n} K^{ij}_{mnmn} : \varepsilon^{*j}_{mn} = \sigma^{\circ}_{mn} \quad \text{for } i = 1, 2, \ldots, n \quad (m, n \text{ not summed}), \tag{73}$$

where $(m, n) = (3, 3)$, $(2, 3)$ or $(3, 1)$,

$$K^{ij}_{3333} = (\beta d_j)\left(\frac{2\mu}{1-\nu}\right)[2s^{11}(i,j) + s^{20}(i,j) + s^{02}(i,j)], \tag{74}$$

$$K^{ij}_{2323} = (\beta d_j)\left(\frac{4\mu}{1-\nu}\right)\left[\left(\frac{1-\nu}{2}\right)s^{10}(i,j) + s^{01}(i,j) - s^{11}(i,j) - s^{02}(i,j)\right], \tag{75}$$

$$K^{ij}_{3131} = (\beta d_j)\left(\frac{4\mu}{1-\nu}\right)\left[s^{10}(i,j)+\left(\frac{1-\nu}{2}\right)s^{01}(i,j)-s^{11}(i,j)-s^{20}(i,j)\right], \tag{76}$$

and $d_j = f_j/\beta$. The infinite series $s^{pq}(i,j)$ are defined by

$$s^{pq}(i,j) = \sum_{\xi}^{\pm\infty\prime} g_j(-\xi)g_i(\xi)(\xi_1^2)^p(\xi_2^2)^q \quad \text{for } p,q = 0,1,2. \tag{77}$$

The analogy between (30)–(32) and (74)–(76) is observed. Usually, it is not easy to calculate the geometrical parameter, g_i, analytically. For example, for a penny-shaped crack with radius c, a numerical scheme must be used in order to calculate

$$g_i(\xi) = \frac{2}{V_1}\int_{r_{i-1}/c}^{r_i/c} r\sqrt{1-r^2}\int_{\theta_{i-1}}^{\theta_i}\cos(\pi n_1(c/a_1)r\cos\theta)\cos(\pi n_2(c/a_2)r\sin\theta)\,\mathrm{d}\theta\,\mathrm{d}r, \tag{78}$$

where

$$V_1 = \tfrac{2}{3}(\theta_i-\theta_{i-1})\left[\sqrt{1-\left(\frac{r_{i-1}}{c}\right)^2}-\sqrt{1-\left(\frac{r_i}{c}\right)^2}\right]; \tag{79}$$

see Fig. 3(a) for notation.

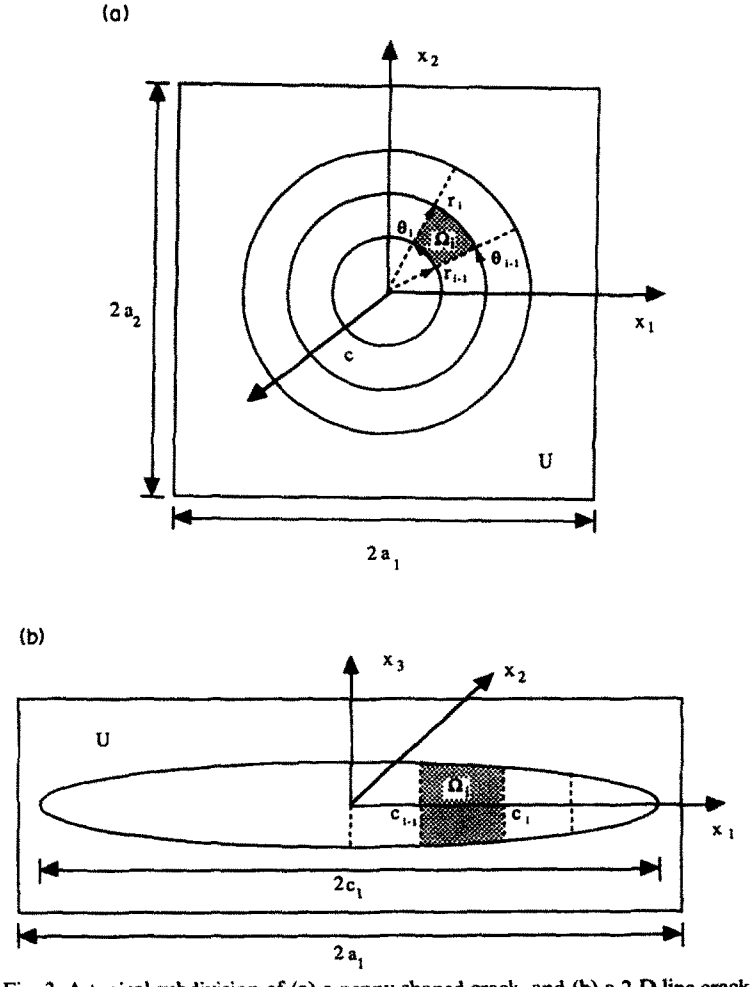

Fig. 3. A typical subdivision of (a) a penny-shaped crack, and (b) a 2-D line crack.

After solving ε^{*j} from (74)–(76), note that the overall compliance tensor, $\bar{\mathbf{D}}$, is given by

$$\bar{\mathbf{D}}:\boldsymbol{\sigma}^{\circ} = \mathbf{D}:\boldsymbol{\sigma}^{\circ} + \sum_{j=1}^{n} (\beta d_j)\varepsilon^{*j}. \tag{80}$$

On the other hand, for periodically distributed 2-D line cracks, eqns (74)–(76) remain the same except that $s^{01}(i,j)$, $s^{11}(i,j)$ and $s^{02}(i,j)$ vanish. The geometry parameter g_i corresponding to Ω_i in Fig. 3(b) is given by, as $\beta \to 0$,

$$g_i(\xi) = \frac{\sin(\pi n_2)}{(\pi n_2)}\left(\frac{2}{V_2}\right)\int_{\varphi_i}^{\varphi_{i-1}} \cos(\pi n_1 (c_1/a_1)\cos\varphi)\sin^2\varphi \, d\varphi, \tag{81}$$

where

$$V_2 = \left(\frac{c_1^i}{c_1}\right)\sqrt{1-\left(\frac{c_1^i}{c_1}\right)^2} - \left(\frac{c_1^{i-1}}{c_1}\right)\sqrt{1-\left(\frac{c_1^{i-1}}{c_1}\right)^2} + \sin^{-1}\left(\frac{c_1^i}{c_1}\right) - \sin^{-1}\left(\frac{c_1^{i-1}}{c_1}\right); \tag{82}$$

$\varphi_i = \cos^{-1}(c_1^i/c_1)$ and $\varphi_{i-1} = \cos^{-1}(c_1^{i-1}/c_1)$.

2.5. *Examples*

The overall moduli of solids containing periodically distributed penny-shaped cracks of radius c_1, are plotted in Fig. 4(a, b) with respect to the crack density parameter f^*, which is defined in (44), i.e.

$$f^* \equiv \lim_{\substack{\beta\to 0\\ f\to 0}} \frac{f}{(\frac{4}{3}\pi)\beta} = \frac{1}{8}\left(\frac{c_1}{a_1}\right)^3 \frac{\alpha}{\gamma_2\gamma_3}. \tag{83}$$

The parameters used are $\alpha\ (=c_2/c_1) = 1$, $\gamma_2\ (=a_2/a_1) = 1$ and $\gamma_3\ (=a_3/a_1) = 0.125$. The parameter γ_3 is chosen such that $f^* = 1$ corresponds to the extreme case when cracks contact each other. The Poisson ratio ν is equal to 0.25. The number of subdivisions used for one quarter of the penny-shaped crack is indicated in the figures. As is seen, the constant eigenstrain assumption is quite good. Indeed, this solution provides an upper bound on the overall moduli (Accorsi and Nemat-Nasser, 1986; Nemat-Nasser *et al.*, 1993). The results are compared with the self-consistent (Hoenig, 1979) and differential scheme (Laws and Dvorak, 1987) solutions of solids with aligned penny-shaped cracks. In Fig. 5(a, b), the results for different crack spacings are compared ($\gamma_3 = 0.125$ and 0.25, respectively). Recall that f^* is defined by (83). Thus, at the same crack density parameter, the solid with fewer cracks (smaller γ_3) contains larger cracks (strictly speaking, larger c_1/a_1) if other parameters are fixed ($\alpha = \gamma_2 = 1$). It is seen from Fig. 5(a, b) that the normalized crack size (c_1/a_1) has a more dominant effect on the stiffness degradation than the effect of crack spacing. In summary, the solid with fewer cracks per unit volume but larger c_1/a_1 is more compliant than the solid with many smaller cracks, even if the crack density parameters are the same. This important *size effect* cannot be modeled by the self-consistent, the differential, and other related methods. The effect of the aspect ratio of elliptical cracks is examined in Fig. 6(a, b). Here $\gamma_3 = 0.125$ is used with $\alpha = \gamma_2 = 1.0$, 0.75, 0.5 and 0.25, respectively. The reason for keeping $\alpha/\gamma_2 = 1$ is to ensure that at the same crack density parameter, the normalized crack size (c_1/a_1) which is a dominant factor, is kept the same. Figure 6(a) shows that as long as the crack size (c_1/a_1) and crack density parameter f^* remain the same, the crack shape has an insignificant effect on the overall Young's modulus. In Fig. 7, the crack spacing is fixed ($\gamma_2 = 1.0$, $\gamma_3 = 0.125$) while the aspect ratio is varied ($\alpha = 0.25$, 0.50, 0.75 and 1.0). The results for periodically distributed 2-D line cracks are illustrated in Fig. 8(a, b, c), where $\gamma_3 = 0.25$ is used. The indicated number of subdivisions is for one half of the crack length. It is again seen that the constant eigenstrain assumption is a good

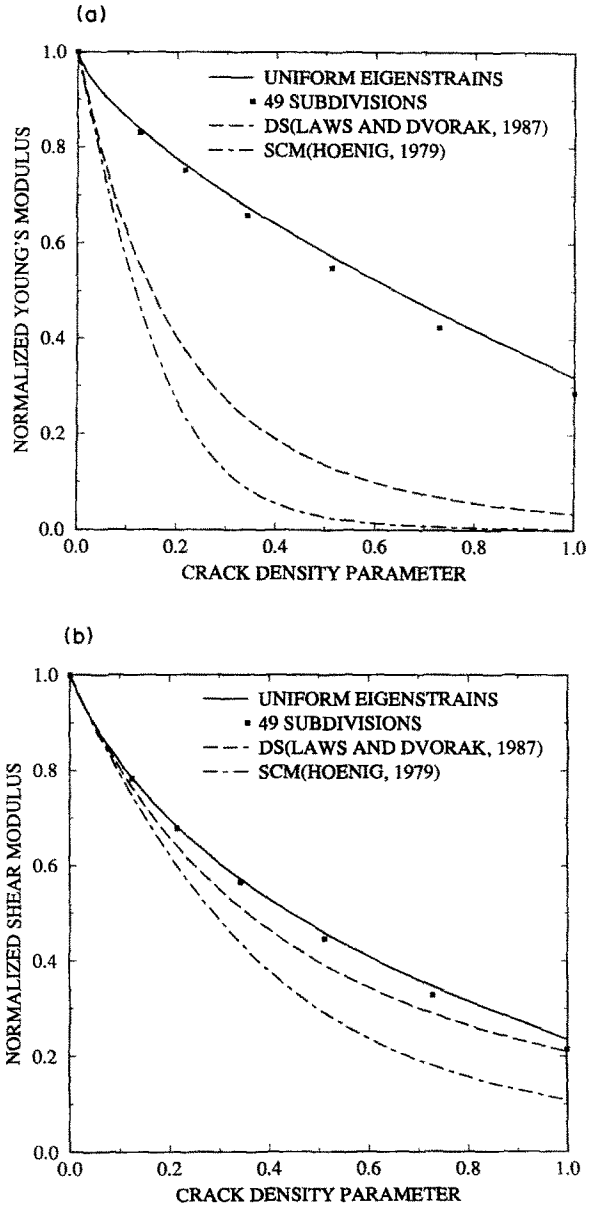

Fig. 4. (a) The normalized Young's modulus $\bar{E}_3/E$, and (b) the normalized shear modulus $\bar{\mu}/\mu$ of solids containing periodically distributed penny-shaped cracks: $a_2/a_1 = 1.0$, $a_3/a_1 = 0.125$; $\nu = 0.25$; also shown are the results obtained by the self-consistent method (Hoenig, 1979) and differential scheme (Laws and Dvorak, 1987).

approximation. At the extreme case when cracks are joining across the adjacent cells ($f^* = c_1/a_1 = 1$), the overall elastic moduli must vanish. The numerical results for these limiting cases yield normalized upper bound moduli of the order of 0.03–0.05, partly as measures of the numerical errors.

The unit cell may contain more than one crack and the crack geometry can be arbitrary; see, for example, Fig. 9(a). In Subsection 2.4, each Ω_i may represent a single crack, or a portion of a crack with a complex geometry. The formulation is still valid, provided that g_i is properly calculated for each Ω_i. As an illustration, consider a unit cell containing two perpendicular 2-D line cracks [Fig. 9(b)]. This kind of microcracking is observed in Mg-PSZ and other ceramics which are subjected to repeated stress pulses in two opposite directions (Subhash and Nemat-Nasser, 1993). In order to account for the interaction between these two cracks, constant but *distinct* eigenstrains ε^{*1} and ε^{*2} are considered for

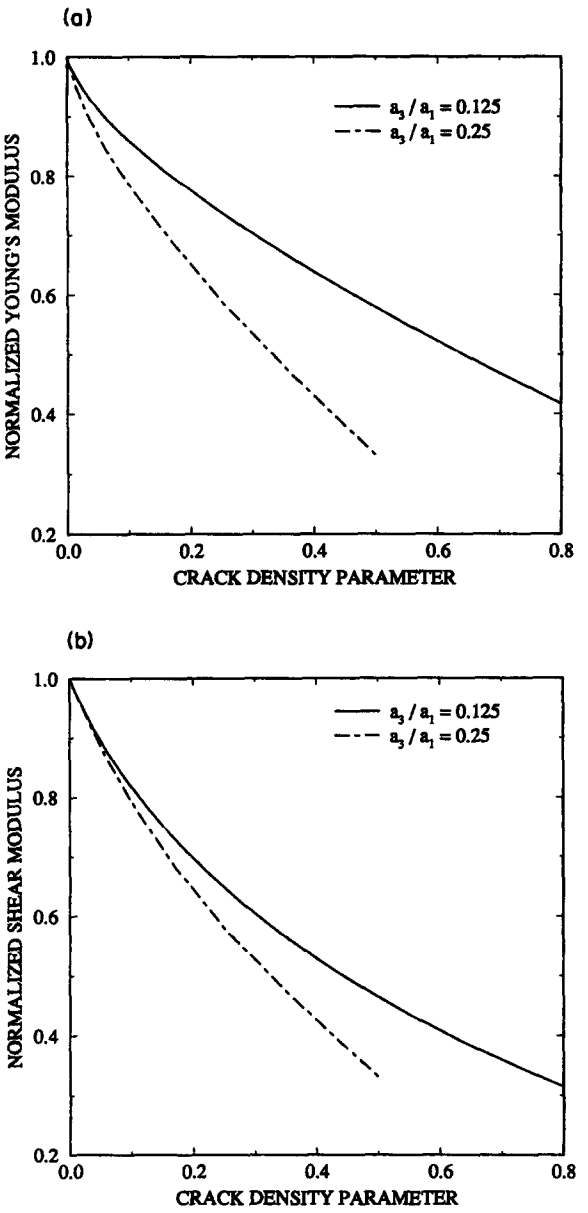

Fig. 5. (a) The normalized Young's modulus $\bar{E}_3/E$, and (b) the normalized shear modulus $\bar{\mu}/\mu$ of solids containing periodically distributed penny-shaped cracks with different crack spacings: $a_3/a_1 = 0.125$ and 0.25, respectively; $a_2/a_1 = 1.0$; $\nu = 0.25$.

homogenization, ε^{*1} in Ω_1 and ε^{*2} in Ω_2. Equations (67) and (68) are still valid. We thus have,

$$\varepsilon^*(\mathbf{x}) = \sum_{j=1}^{2} H(\Omega_j)\varepsilon^{*j}, \tag{84}$$

$$\langle \varepsilon^p(\mathbf{x})\rangle_{\Omega_i} = \sum_{j=1}^{2} f_i \sum_{\xi}^{\pm\infty\prime} g_j(-\xi)g_i(\xi)\hat{\mathbf{S}}(\xi) : \varepsilon^{*j} \quad \text{for } i = 1, 2. \tag{85}$$

The consistency conditions yield

$$\sigma^\circ + \langle \sigma^p(\mathbf{x})\rangle_{\Omega_i} = \mathbf{0} \quad \text{in } \Omega_i \ (i = 1, 2), \tag{86}$$

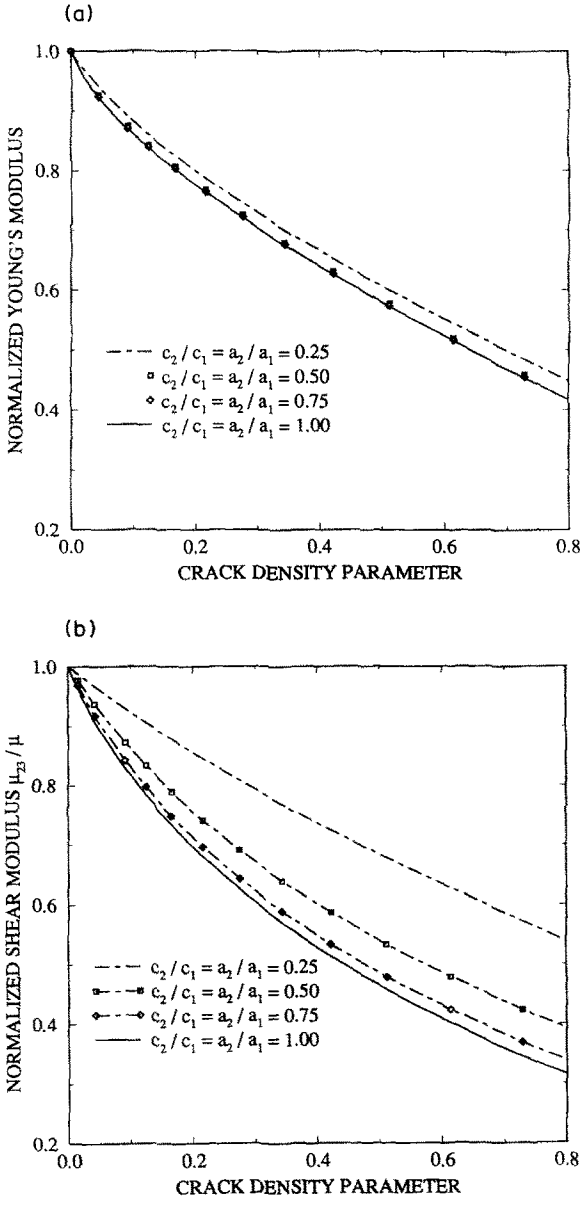

Fig. 6. (a) The normalized Young's modulus $\bar{E}_3/E$, and (b) the normalized shear modulus $\bar{\mu}_{23}/\mu$ of solids containing periodically elliptic cracks with different aspect ratios and crack spacings: $c_2/c_1 = a_2/a_1 = 0.25, 0.50, 0.75$ and 0.1, respectively; $a_3/a_1 = 0.125$; $\nu = 0.25$.

from which the necessary eigenstrains for homogenization are given by

$$\boldsymbol{\varepsilon}^{*i} = \mathbf{M}^i : \boldsymbol{\sigma}^\circ \quad \text{for } i = 1, 2, \tag{87}$$

where

$$\mathbf{M}^1 = \{[(1-f_1)\mathbf{1}^{(4s)} - f_1\bar{\mathbf{S}}^{11}] - f_2(\mathbf{1}^{(4s)} + \bar{\mathbf{S}}^{12}) : [(1-f_2)\mathbf{1}^{(4s)} - f_2\bar{\mathbf{S}}^{22}]^{-1} : f_1(\mathbf{1}^{(4s)} + \bar{\mathbf{S}}^{12})\}^{-1} : \{\mathbf{1}^{(4s)} + f_2(\mathbf{1}^{(4s)} + \bar{\mathbf{S}}^{12}) : [(1-f_2)\mathbf{1}^{(4s)} - f_2\bar{\mathbf{S}}^{22}]^{-1}\} : \mathbf{D}, \tag{88}$$

$$\mathbf{M}^2 = \{[(1-f_2)\mathbf{1}^{(4s)} - f_2\bar{\mathbf{S}}^{22}] - f_1(\mathbf{1}^{(4s)} + \bar{\mathbf{S}}^{12}) : [(1-f_1)\mathbf{1}^{(4s)} - f_1\bar{\mathbf{S}}^{11}]^{-1} : f_2(\mathbf{1}^{(4s)} + \bar{\mathbf{S}}^{12})\}^{-1} : \{\mathbf{1}^{(4s)} + f_1(\mathbf{1}^{(4s)} + \bar{\mathbf{S}}^{12}) : [(1-f_1)\mathbf{1}^{(4s)} - f_1\bar{\mathbf{S}}^{11}]^{-1}\} : \mathbf{D}, \tag{89}$$

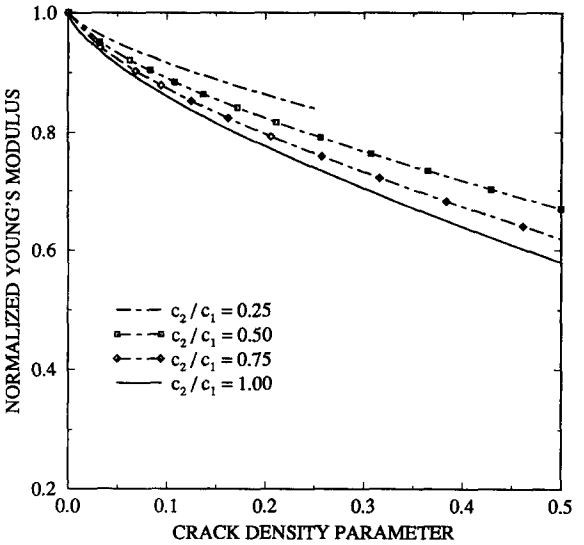

Fig. 7. The normalized Young's modulus $\bar{E}_3/E$ of solids containing periodically distributed elliptic cracks with different aspect ratios: $c_2/c_1 = 0.25, 0.50, 0.75$ and 1.0, respectively. The crack spacings are fixed at $a_2/a_1 = 1.0$, $a_3/a_1 = 0.125$; $\nu = 0.25$.

where

$$\bar{\mathbf{S}}^{ij} = \sum_{\xi}^{\pm\infty\prime} g_i(\xi) g_j(-\xi) \hat{\mathbf{S}}(\xi) \quad \text{for } i,j = 1,2. \tag{90}$$

Observe that the above formulation is really a special case of $\Omega = \Omega_1 \cup \Omega_2$ for the piecewise constant eigenstrain formulation discussed in Subsection 2.4. However, each crack is associated with its own geometric parameter given by $g_i(\xi)$. For the unit cell containing two perpendicular 2-D line cracks shown in Fig. 9(b), the geometrical parameters are given by

$$g_1(\xi) = 2\cos(\xi_1\delta_1)\cos(\xi_3\delta_2)\frac{J_1(b\xi_1)}{(b\xi_1)}\frac{\sin(\pi n_2)}{(\pi n_2)}, \tag{91a}$$

$$g_2(\xi) = 2\cos(\xi_1\delta_3)\cos(\xi_3\delta_4)\frac{J_1(c\xi_3)}{(c\xi_3)}\frac{\sin(\pi n_2)}{(\pi n_2)}, \tag{91b}$$

where $2b$ and $2c$ are the crack lengths of Ω_1 and Ω_2, respectively. As long as the two cracks are perpendicular to each other, the stiffness degradation of overall anti-plane shear moduli $\bar{\mu}_{23}$ and $\bar{\mu}_{12}$ are affected only by the crack parallel to the x_1- and x_3-axes, respectively. However, the overall Young moduli $\bar{E}_1$ and $\bar{E}_3$, and the in-plane shear modulus $\bar{\mu}_{31}$ are affected by both cracks. A calculation similar to (but somewhat more complicated than) that presented in Subsection 2.2, now yields

$$\bar{E}_1/E = \{1+[(1-\nu^2)s^2][s^2s^4-(s^5-s^6)(s^7-s^8)]^{-1}\}^{-1}, \tag{92}$$

$$\bar{E}_3/E = \{1+[(1-\nu^2)s^4][s^2s^4-(s^5-s^6)(s^7-s^8)]^{-1}\}^{-1}, \tag{93}$$

$$\bar{\mu}_{31}/\mu = \left\{1+\left(\frac{1-\nu}{2}\right)\{[1-(s^5-s^6)(s^1-s^2)^{-1}][(s^3-s^4)-(s^5-s^6)(s^7-s^8)(s^1-s^2)^{-1}]^{-1} + [1-(s^7-s^8)(s^3-s^4)^{-1}][(s^1-s^2)-(s^5-s^6)(s^7-s^8)(s^3-s^4)^{-1}]^{-1}\}\right\}^{-1}, \tag{94}$$

where the notation in (77) is changed as follows: $s^1 = s^{10}(1,1)$, $s^2 = s^{20}(1,1)$, $s_3 = s^{01}(2,2)$, $s^4 = s^{02}(2,2)$, $s^5 = s^{10}(1,2)$, $s^6 = s^{20}(1,2)$, $s^7 = s^{01}(1,2)$ and $s^8 = s^{02}(1,2)$. The results for the case of $\delta_1 = \delta_2 = \delta_4 = 0$, $\delta_3 = a_1$ and $\gamma_3 = 0.25$ are shown in Fig. 10. Comparison of Fig. 8(a, b) and Fig. 10 shows the interaction effects.

3. CRACK OPENING DISPLACEMENTS AND STRESS INTENSITY FACTORS

Before studying the COD of periodically distributed cracks, we consider an infinitely extended linearly elastic solid containing a single flat ellipsoidal void, Ω, with semi-axes $c_1 \geqslant c_2 > c_3$. The infinite medium is subjected to a homogeneous strain field $\boldsymbol{\varepsilon}^\circ$ at infinity. Eshelby (1957) has shown that after homogenization, the disturbance strain field within the void is constant and can be expressed by $\boldsymbol{\varepsilon}^d = \mathbf{S} : \boldsymbol{\varepsilon}^*$ where $\mathbf{S}$ is a fourth-order constant tensor and $\boldsymbol{\varepsilon}^*$ is the constant eigenstrain introduced for homogenization.

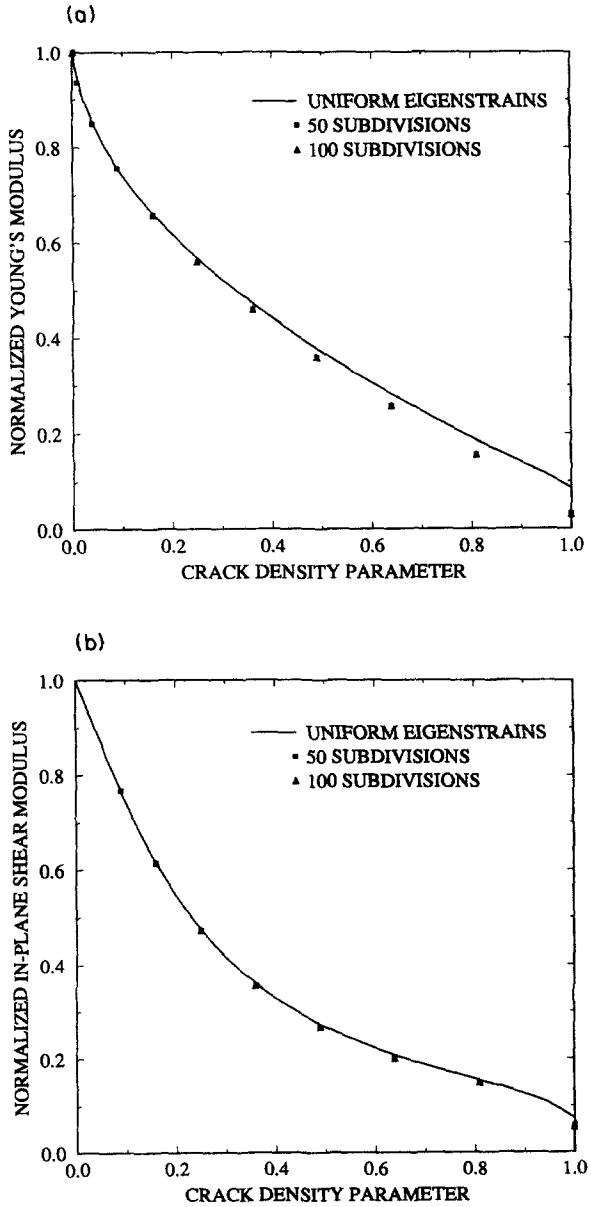

Fig. 8. (a) The normalized Young's modulus $\bar{E}_3/E$, and (b) the normalized in-plane shear modulus $\bar{\mu}_{31}/\mu$, (c) the normalized anti-plane shear modulus $\bar{\mu}_{23}/\mu$ of solids with periodically distributed 2-D line cracks: $a_2/a_1 = 0.25$; $\nu = 0.25$.

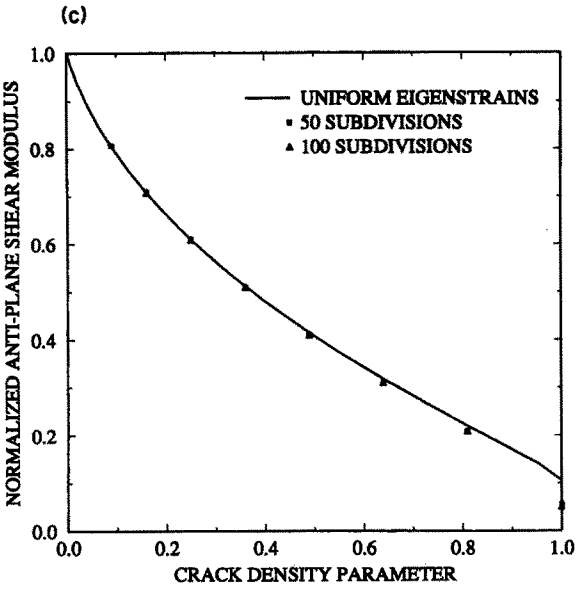

Fig. 8 (*continued*).

As pointed out before, when β $(=c_3/c_1)$ approaches zero, the flat ellipsoidal void collapses into an elliptic crack. The traction-free condition on the crack faces requires the following consistency condition:

$$\sigma(\mathbf{x}) = \mathbf{C}:(\varepsilon^{\circ}+\mathbf{S}:\varepsilon^{*}-\varepsilon^{*}) = \mathbf{0} \quad \text{in } \Omega. \tag{95}$$

Or equivalently,

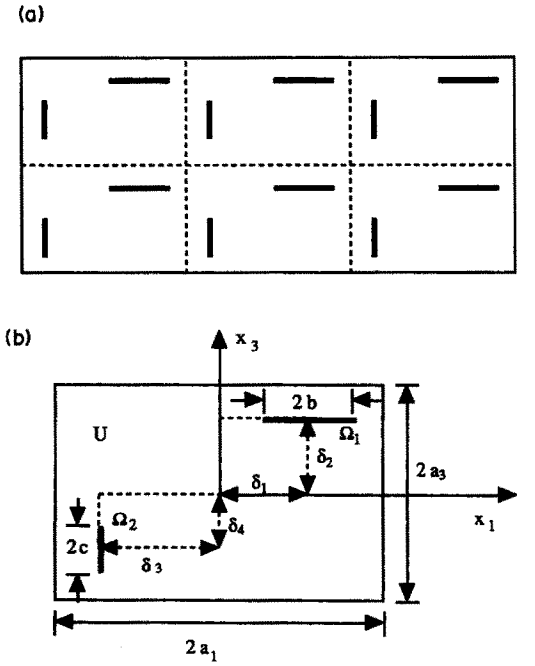

Fig. 9. (a) Solids with periodically distributed perpendicular 2-D line cracks, and (b) unit cell containing two perpendicular 2-D line cracks.

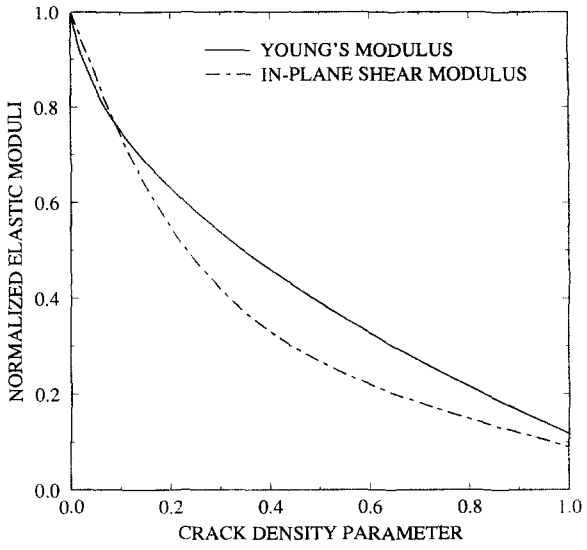

Fig. 10. The normalized Young's modulus $\bar{E}/E$ and the normalized in-plane shear modulus $\bar{\mu}_{31}/\mu$ of solids with periodically distributed perpendicular 2-D line cracks.

$$\varepsilon^* = \frac{1}{\beta}\mathbf{U}^{-1}:\boldsymbol{\sigma}^\circ, \tag{96}$$

where

$$\mathbf{U}^{-1} = \beta(\mathbf{C}-\mathbf{C}:\mathbf{S})^{-1}, \tag{97}$$

and $\boldsymbol{\sigma}^\circ = \mathbf{C}:\boldsymbol{\varepsilon}^\circ$ is the corresponding homogeneous stress field. Substitution of $\mathbf{S}$ for penny-shaped and elliptic-cylindrical inclusions [see, for example, Mura (1987)] into (97) yields

$$U^{-1}_{3333} = \beta(C-C:S)^{-1}_{3333} = \frac{4(1-\nu^2)}{\pi E}, \tag{98}$$

$$U^{-1}_{2323} = U^{-1}_{3131} = \frac{(1-\nu)}{\pi\mu(2-\nu)}, \tag{99}$$

for the penny-shaped crack, and

$$U^{-1}_{3333} = \frac{2(1-\nu^2)}{E}, \tag{100}$$

$$U^{-1}_{2323} = \frac{1}{4\mu}, \tag{101}$$

$$U^{-1}_{3131} = \frac{1-\nu}{4}, \tag{102}$$

for the 2-D line crack.

Since the strain field within Ω is uniform, the corresponding displacement field is given by

$$\mathbf{u}(\mathbf{x}) = \mathbf{x}\cdot(\boldsymbol{\varepsilon}^\circ + \boldsymbol{\varepsilon}^{\mathrm{d}}) = \mathbf{x}\cdot\boldsymbol{\varepsilon}^*, \tag{103}$$

where (95) is used. In view of the fact that

$$x_3 = \pm \beta c_1 \sqrt{1 - \left(\frac{x_1}{c_1}\right)^2 - \left(\frac{x_2}{c_2}\right)^2} \tag{104}$$

on the crack surfaces, and with the aid of (96), (103) and (104), the COD is given by:

$$[u_3] = 2c_1 \sqrt{1 - \left(\frac{x_1}{c_1}\right)^2 - \left(\frac{x_2}{c_2}\right)^2}\, U^{-1}_{3333}\sigma^\circ_{33}, \tag{105a}$$

$$[u_i] = 4c_1 \sqrt{1 - \left(\frac{x_1}{c_1}\right)^2 - \left(\frac{x_2}{c_2}\right)^2}\, U^{-1}_{3i3i}\sigma^\circ_{3i} \quad \text{for } i = 1, 2 \ (i \text{ not summed}). \tag{105b}$$

One can apply the above technique to the case of periodically distributed cracks. Recalling that (23) and (24) give

$$\boldsymbol{\varepsilon}^{*\circ} = \frac{1}{\beta}(\mathbf{U}^{\mathrm{p}})^{-1} : \boldsymbol{\sigma}^\circ, \tag{106}$$

where

$$(\mathbf{U}^{\mathrm{p}})^{-1} = \beta \left[(1-f)\mathbf{C} - \sum_{\xi}^{\pm\infty\prime} fg(\xi)g(-\xi)\mathbf{C} : \hat{\mathbf{S}}(\xi) \right]^{-1}. \tag{107}$$

Thus, one obtains

$$[u_3] = 2c_1 \sqrt{1 - \left(\frac{x_1}{c_1}\right)^2 - \left(\frac{x_2}{c_2}\right)^2}\, (U^{\mathrm{p}})^{-1}_{3333}\sigma^\circ_{33}, \tag{108a}$$

$$[u_i] = 4c_1 \sqrt{1 - \left(\frac{x_1}{c_1}\right)^2 - \left(\frac{x_2}{c_2}\right)^2}\, (U^{\mathrm{p}})^{-1}_{3i3i}\sigma^\circ_{3i} \quad \text{for } i = 1, 2 \ (i \text{ not summed}). \tag{108b}$$

For 2-D line cracks, the same conclusion is expected, except that $[1-(x_1/c_1)^2-(x_2/c_2)^2]^{1/2}$ is replaced by $[1-(x_1/c_1)^2]^{1/2}$. Furthermore, one observes that the coefficient of COD is proportional to the stress intensity factor [for example, see Irwin (1962)]. Hence, the SIF for periodically distributed cracks, K^{p} (normalized by K which is the SIF of a single crack embedded in an infinite homogeneous body), is given by

$$\left(\frac{K^{\mathrm{p}}_{\mathrm{I}}}{K_{\mathrm{I}}}, \frac{K^{\mathrm{p}}_{\mathrm{II}}}{K_{\mathrm{II}}}, \frac{K^{\mathrm{p}}_{\mathrm{III}}}{K_{\mathrm{III}}}\right) = \left(\frac{(U^{\mathrm{p}})^{-1}_{3333}}{U^{-1}_{3333}}, \frac{(U^{\mathrm{p}})^{-1}_{3131}}{U^{-1}_{3131}}, \frac{(U^{\mathrm{p}})^{-1}_{2323}}{U^{-1}_{2323}}\right), \tag{109}$$

for Modes I, II, III, respectively, where, from (30)–(32),

$$(U^{\mathrm{p}})^{-1}_{3333} = \frac{1}{d}\left(\frac{1-\nu^2}{E}\right)(s^{20} + 2s^{11} + s^{02})^{-1}, \tag{110}$$

$$(U^{\mathrm{p}})^{-1}_{3131} = \frac{1}{d}\left(\frac{1}{4\mu}\right)\left[s^{01} + \left(\frac{2}{1-\nu}\right)(s^{10} - s^{11} - s^{20})\right]^{-1}, \tag{111}$$

$$(U^{\mathrm{p}})^{-1}_{2323} = \frac{1}{d}\left(\frac{1}{4\mu}\right)\left[s^{10} + \left(\frac{2}{1-\nu}\right)(s^{01} - s^{11} - s^{02})\right]^{-1}, \tag{112}$$

for both elliptic and 2-D line cracks. For the latter, s^{01}, s^{11} and s^{02} vanish. However, we must point out that (109) is an approximation in the sense that uniform eigenstrain $\boldsymbol{\varepsilon}^*$ is

assumed within Ω, or, the average value, $\langle \boldsymbol{\varepsilon}^*(\mathbf{x})\rangle_\Omega$, is used instead of $\boldsymbol{\varepsilon}^*(\mathbf{x})$. Thus, K^p is the average of SIF taken along the crack edge.

4. CONCLUSIONS AND DISCUSSIONS

The formulation presented in this work is *internally* consistent in the sense that, if instead of the homogeneous stress $\boldsymbol{\sigma}^\circ$, the homogeneous strain $\boldsymbol{\varepsilon}^\circ$ is applied, the overall elasticity tensor, $\bar{\mathbf{C}}$, defined by

$$\langle \boldsymbol{\sigma}(\mathbf{x})\rangle_U = \boldsymbol{\sigma}^\circ = \bar{\mathbf{C}} : \boldsymbol{\varepsilon}^\circ, \tag{113}$$

will be the inverse of $\bar{\mathbf{D}}$ (Nemat-Nasser *et al.*, 1982).

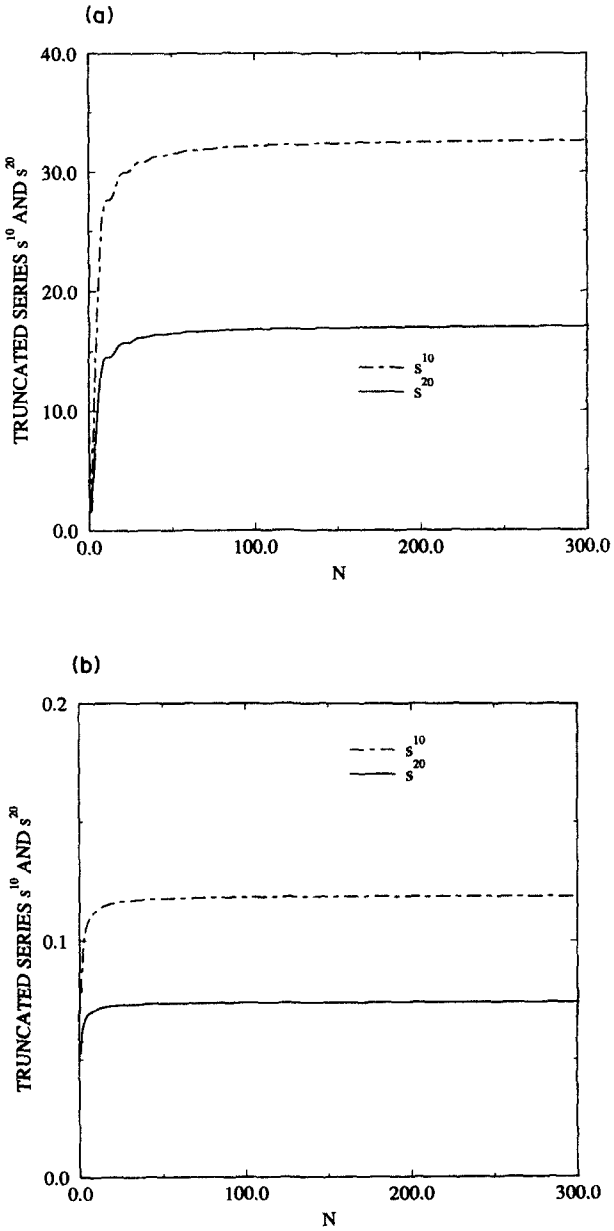

Fig. 11. The truncated infinite series s^{10} and s^{20} of periodically distributed 2-D line cracks at (a) low crack density, $f^* = 0.01$ ($c_1/a_1 = 0.1$), and (b) high crack density, $f^* = 1.0$ ($c_1/a_1 = 1.0$); $a_3/a_1 = 0.25$.

The formulation can also be presented in terms of an eigenstress field, $\sigma^*(\mathbf{x})$, instead of an eigenstrain field (Nemat-Nasser and Hori, 1988, 1993). It can be easily shown that $\varepsilon^*(\mathbf{x})$ and $\sigma^*(\mathbf{x})$ are related through

$$\sigma^*(\mathbf{x}) = -\mathbf{C} : \varepsilon^*(\mathbf{x}). \tag{114}$$

Since both the geometry and the elastic properties of cracked solids are assumed to be periodic functions of the space variable, $\mathbf{x}$, the Fourier series expansions of the elastic fields are *exact*. Only one approximation is involved in this formulation, i.e. the distribution of eigenstrain, which is assumed to be piecewise constant. It is seen in Subsection 2.5, that the uniform eigenstrain assumption is a good approximation over a broad range of crack density parameters.

It is also noted that in (21) the effect of geometry (the g-parameter) is uncoupled from that of the elastic properties (the $\hat{\mathbf{S}}$-tensor). Therefore, the formulation for elliptic cracks, 2-D line cracks, and cracks with arbitrary shapes is basically the same provided that the corresponding $g(\xi)$ is properly calculated. Furthermore since this model takes into account the crack geometry and distribution precisely, it may be applied to study the process of fragmentation by crack coalescence.

Finally, the estimate of the overall elasticity or compliance tensor actually is equivalent to the determination of the average eigenstrains, $\langle \varepsilon^*(\mathbf{x}) \rangle_U$, as pointed out in Subsection 2.1. The problem further reduces to the calculation of several infinite series s^{pq} ($p, q = 0, 1, 2$). The convergence characteristics of these infinite series are illustrated in Fig. 11 for the case of periodic 2-D line cracks along with uniform eigenstrain assumption. It is seen that the series converge rapidly at either low or high crack densities. Thus the truncation errors and possible round-off errors should be negligible.

Acknowledgements—This work was supported by the U.S. Army Research Office under Grant DAAL-03-86-K-0169 to the University of California, San Diego. The computations were carried out at the San Diego Supercomputer Center.

REFERENCES

Aboudi, J. and Benveniste, Y. (1987). The effective moduli of cracked bodies in plane deformations. *Engng Fract. Mech.* **26**(2), 171–184.

Accorsi, M. L. and Nemat-Nasser, S. (1986). Bounds on the overall elastic and instantaneous elastoplastic moduli of periodic composites. *Mech. Mater.* **5**, 209–220.

Benveniste, Y. (1986). On the Mori–Tanaka's method in cracked bodies. *Mech. Res. Comm.* **13**(4), 193–201.

Bristow, J. R. (1960). Microcracks, and the static and dynamic elastic constants of annealed and heavily cold-worked metals. *Brit. J. Appl. Phys.* **11**, 81–85.

Bruner, W. M. (1976). Comment on "Seismic velocities in dry and saturated cracked solids" by Richard J. O'Connell and Bernard Budiansky. *J. Geophys. Res.* **81**(14), 2573–2576.

Budiansky, B. and O'Connell, R. J. (1976). Elastic moduli of a cracked solid. *Int. J. Solids Structures* **12**, 81–97.

Christensen, R. M. (1990). A critical evaluation for a class of micromechanics models. *J. Mech. Phys. Solids* **38**(3), 379–404.

Christensen, R. M. and Lo, K. H. (1979). Solutions for effective shear properties in three phase sphere and cylinder models. *J. Mech. Phys. Solids* **27**, 315–330.

Christensen, R. M. and Lo, K. H. (1986). Erratum: Solutions for effective shear properties in three phase sphere and cylinder models. *J. Mech. Phys. Solids* **34**(6), 639.

Delameter, W. R., Herrmann, G. and Barnett, D. M. (1975). Weakening of an elastic solid by a rectangular array of cracks. *J. Appl. Mech.* **42**(1), 74–80.

Delameter, W. R., Herrmann, G. and Barnett, D. M. (1977). Erratum. *J. Appl. Mech.* **44**(1), 190.

Deng, H. and Nemat-Nasser, S. (1992). Microcrack arrays in isotropic solids. *Mech. Mater.* **13**(1), 15–36.

Eshelby, J. D. (1957). The determination of the elastic field of an ellipsoidal inclusion, and related problems. *Proc. R. Soc.* **A241**, 376–396.

Fröhlich, H. and Sack, R. (1946). Theory of the rheological properties of dispersions. *Proc. R. Soc.* **A185**, 415–430.

Hashin, Z. (1988). The differential scheme and its application to cracked materials. *J. Mech. Phys. Solids* **36**(6), 719–734.

Henyey, F. S. and Pomphrey, N. (1982). Self-consistent elastic moduli of a cracked solid. *Geophys. Res. Lett.* **9**(8), 903–906.

Hermans, J. J. (1967). The elastic properties of fiber reinforced materials when the fibers are aligned. *Proc. K. Ned. Akad. Wet.* **B70**, 1–9.

Hoenig, A. (1979). Elastic moduli of a non-randomly cracked body. *Int. J. Solids Structures* **15**, 137–154.

Horii, H. and Nemat-Nasser, S. (1983). Overall moduli of solids with microcracks: load-induced anisotropy. *J. Mech. Phys. Solids* **31**(2), 155–171.

Horii, H. and Sahasakmontri, K. (1990). Mechanical properties of cracked solids: validity of the self-consistent method. In *Micromechanics and Inhomogeneity. The Toshio Mura Anniversary Volume* (Edited by G. J. Weng, M. Taya and H. Abé), pp. 137–159. Springer, New York.

Hudson, J. A. (1980). Overall properties of a cracked solid. *Math. Proc. Camb. Phil. Soc.* **88,** 371–384.

Hudson, J. A. (1990). Overall elastic properties of isotropic materials with arbitrary distribution of circular cracks. *Geophys. Jl Int.* **102,** 465–469.

Hudson, J. A. and Knopoff, L. (1989). Predicting the overall properties of composite materials with small-scale inclusions or cracks. *PAGEOPH.* **131**(4), 551–576.

Irwin, G. R. (1962). Crack-extension force for a part-through crack in a plate. *J. Appl. Mech.* **29**(4), 651–654.

Iwakuma, T. and Nemat-Nasser, S. (1983). Composites with periodic microstructure. *Comput. Struct.* **16**(1–4), 13–19.

Kerner, E. H. (1956). The elastic and thermo-elastic properties of composite media. *Proc. Phys. Soc.* **69B,** 808–813.

Laws, N. and Brockenbrough, J. R. (1987). The effect of micro-crack systems on the loss of stiffness of brittle solids. *Int. J. Solids Structures* **23**(9), 1247–1268.

Laws, N. and Dvorak, G. J. (1987). The effect of fiber breaks and aligned penny-shaped cracks on the stiffness and energy release rates in unidirectional composites. *Int. J. Solids Structures* **23**(9), 1269–1283.

Mackenzie, J. K. (1950). The elastic constants of a solid containing spherical holes. *Proc. Phys. Soc.* **B63,** 2–11.

Mori, T. and Tanaka, K. (1973). Average stress in matrix and average elastic energy of materials with misfitting inclusions. *Acta Metall.* **21,** 571–574.

Mura, T. (1987). *Micromechanics of Defects in Solids* (2nd edn, rev.). Martinus Nijhoff, Dordrecht, The Netherlands.

Nemat-Nasser, S. and Hori, M. (1988). Micromechanics: Overall properties of heterogeneous elastic solids. UCSD class notes.

Nemat-Nasser, S. and Hori, M. (1990). Elastic solids with microdefects. In *Micromechanics and Inhomogeneity. The Toshio Mura Anniversary Volume* (Edited by G. J. Weng, M. Taya and H. Abé), pp. 297–320. Springer, New York.

Nemat-Nasser, S. and Hori, M. (1993). *Micromechanics: Overall Properties of Heterogeneous Solids.* Elsevier Science Publishers, North-Holland.

Nemat-Nasser, S., Iwakuma, T. and Hejazi, M. (1982). On composites with periodic structure. *Mech. Mater.* **1,** 239–267.

Nemat-Nasser, S. and Taya, M. (1981). On effective moduli of an elastic body containing periodically distributed voids. *Q. Appl. Math.* **39,** 43–59.

Nemat-Nasser, S. and Taya, M. (1985). On effective moduli of an elastic body containing periodically distributed voids: comments and corrections. *Q. Appl. Math.* **43,** 187–188.

Nemat-Nasser, S., Yu, N. and Hori, M. (1993). Bounds and estimates of overall moduli of composites with periodic microstructure. *Mech. Mater.* (submitted).

O'Connell, R. J. and Budiansky, B. (1974). Seismic velocities in dry and saturated cracked solids. *J. Geophys. Res.* **79**(35), 5412–5426.

van der Poel, C. (1958). On the rheology of concentrated dispersions. *Rheol. Acta* **1**(2–3), 198–205.

Salganik, R. L. (1973). Mechanics of bodies with many cracks. *Izv. AN SSSR. Mekhanika Tverdogo Tela* **8**(4), 149–158 (English translation, *Mech. Solids* **8,** 135–143).

Smith, J. C. (1974). Correction and extension of van der Poel's method for calculating the shear modulus of a particular composite. *J. Res. Nat. Bur. Stand.* **78A**(3), 355–361.

Smith, J. C. (1975). Simplification of van der Poel's formula for the shear modulus of a particulate composite. *J. Res. Nat. Bur. Stand.* **79A**(2), 419–423.

Subhash, G. and Nemat-Nasser, S. (1993). Dynamic stress-induced transformation and texture formation in uniaxial compression of zirconia ceramics. *J. Am. Cer. Soc.* **76**(1), 153–165.

Walsh, J. B. (1969). New analysis of attenuation in partially melted rock. *J. Geophys. Res.* **74**(17), 4333–4337.

Willis, J. R. (1980a). A polarization approach to the scattering of elastic waves—I. Scattering by a single inclusion. *J. Mech. Phys. Solids* **28,** 287–305.

Willis, J. R. (1980b). A polarization approach to the scattering of elastic waves—II. Multiple scattering from inclusions. *J. Mech. Phys. Solids* **28,** 307–327.

APPENDIX

The response of a periodic structure is not necessarily periodic if arbitrary boundary conditions are prescribed on the surfaces of the unit cells. In the recent work of Nemat-Nasser and Hori (1988, 1993), the technique of *mirror-image decomposition* of periodic fields has been introduced to examine this and related issues. The periodic elastic fields associated with solids of periodic microstructure, and the corresponding boundary conditions for the unit cell can be systematically decomposed into symmetric and antisymmetric fields, using a sequence of mirror-image reflections with respect to the coordinate planes. In view of the periodicity and mirror-image symmetry/antisymmetry, Nemat-Nasser and Hori (1988, 1993) conclude for a parallelepiped unit cell that as long as the geometry and elastic properties of the unit cell are completely symmetric with respect to all three rectangular Cartesian coordinate planes, the boundary conditions of the unit cell must be either

$$\mathbf{u}^n = \mathbf{t}^t = \mathbf{0} \quad \text{or} \quad \mathbf{t}^n = \mathbf{u}^t = \mathbf{0}, \tag{A1}$$

where the normal and tangential components of the displacements and tractions are

$$\mathbf{u}^n = (\boldsymbol{\nu}\cdot\mathbf{u})\boldsymbol{\nu}, \quad \mathbf{u}^t = \mathbf{u} - \mathbf{u}^n, \tag{A2a}$$

$$\mathbf{t}^n = (\boldsymbol{\nu}\cdot\mathbf{t})\boldsymbol{\nu}, \quad \mathbf{t}^t = \mathbf{t} - \mathbf{t}^n, \tag{A2b}$$

with ν being the unit normal of the unit cell boundary. If the homogeneous stress field σ° is applied, then the following conditions should be prescribed on the boundary surfaces of the unit cell:

(1) σ°_{ii} is applied ($i = 1, 2, 3$, i not summed):

$$\mathbf{u}^n = \mathbf{u}^{\circ n} \quad \text{and} \quad \mathbf{t}^t = \mathbf{t}^{\circ t} \quad \text{on } x_i = \pm a_i. \tag{A3}$$

(2) σ°_{23} is applied:

$$\mathbf{u}^n = \mathbf{u}^{\circ n} \quad \text{and} \quad \mathbf{t}^t = \mathbf{t}^{\circ t} \quad \text{on } x_1 = \pm a_1, \tag{A4a}$$

$$\mathbf{u}^t = \mathbf{u}^{\circ t} \quad \text{and} \quad \mathbf{t}^n = \mathbf{t}^{\circ n} \quad \text{on } x_i = \pm a_i \quad \text{for } i = 2, 3. \tag{A4b}$$

(3) σ°_{31} is applied:

$$\mathbf{u}^n = \mathbf{u}^{\circ n} \quad \text{and} \quad \mathbf{t}^t = \mathbf{t}^{\circ t} \quad \text{on } x_2 = \pm a_2, \tag{A5a}$$

$$\mathbf{u}^t = \mathbf{u}^{\circ t} \quad \text{and} \quad \mathbf{t}^n = \mathbf{t}^{\circ n} \quad \text{on } x_i = \pm a_i \quad \text{for } i = 1, 3. \tag{A5b}$$

(4) σ°_{12} is applied:

$$\mathbf{u}^n = \mathbf{u}^{\circ n} \quad \text{and} \quad \mathbf{t}^t = \mathbf{t}^{\circ t} \quad \text{on } x_3 = \pm a_3, \tag{A6a}$$

$$\mathbf{u}^t = \mathbf{u}^{\circ t} \quad \text{and} \quad \mathbf{t}^n = \mathbf{t}^{\circ n} \quad \text{on } x_i = \pm a_i \quad \text{for } i = 1, 2, \tag{A6b}$$

where $\mathbf{t}^\circ = \nu \cdot \sigma^\circ$, and $\mathbf{u}^\circ = \mathbf{x} \cdot \varepsilon^\circ$. Here, $\mathbf{u}^{\circ n}$, $\mathbf{u}^{\circ t}$, $\mathbf{t}^{\circ n}$ and $\mathbf{t}^{\circ t}$ are defined in the same way as (A2a, b). Since the homogeneous strain ε° is related to the applied homogeneous stress σ° through $\bar{\mathbf{D}}$, then if σ° is applied, the displacement boundary data remain to be determined by the solution, since the corresponding ε° is not known until $\bar{\mathbf{D}}$ is determined.